# Electronic structure of $Na_3Sb$ and $Na_2KSb$

A. R. H. F. Ettema*
*Delft Institute for Microelectronics and Submicrontechnology, Delft University of Technology, Department of Physics, Lorentzweg 1, 2628 CJ Delft, The Netherlands*

R. A. de Groot
*Research Institute of Materials, University of Nijmegen, Department of Physics, Toernooiveld 1, 6525 ED Nijmegen, The Netherlands*
(Received 23 July 1999)

The photoemissive materials $Na_3Sb$ and $Na_2KSb$ are widely applied as photocathodes in light detection devices. Their application is purely electronic, therefore results from band-structure calculations are important to understand the photon-electron conversion in the cathodes of these devices. This study reports results from band-structure calculations for $Na_3Sb$ and $Na_2KSb$. These calculations show that the monoalkali antimonide has a small band gap with respect to the photon absorption onset. For the bialkali antimonide the discrepancy between the band gap and the photon absorption onset is significantly smaller. Therefore the photoelectrons in the monoalkali antimonide have a higher escape barrier than those in the bialkali antimonide. This is likely the reason for the higher emission rates of the bialkali antimonide $Na_2KSb$.

## I. INTRODUCTION

The alkali antimonides are compounds that are widely used as photocathode materials. Their good characteristics regarding photon absorption and work function are the main reasons for their successful use in electron emission devices.[1,2] In order to obtain more understanding of the electronic mechanisms in the application of these materials more information is needed about their band structure.

A general overview of the band structure of alkali pnictide compounds has been given by Tegze and Hafner.[3] They used the linear muffin-tin orbital (LMTO) method to calculate the energy bands of various binary alkali pnictide compounds with different stoichiometries and crystal structures. Their results are discussed in relation to the phase diagrams of the compounds and the electrical transport properties of the molten alloys. A more comprehensive study has been given by Chulkov, Koroleva, and Silkin.[4] They performed a first-principles calculation based on pseudopotentials, including scalar relativistic effects and spin-orbit splitting, in order to obtain the band-gap values of several alkali antimonide and alkali bismuthide compounds. The calculated band gaps are found to be underestimated with respect to the experimental values, but provide an overview of the order of magnitude of the band gaps in various alkali antimonides. Wei and Zunger[5] calculated the band structures and total energies for $Li_3Sb$, $K_3Sb$, and $Cs_3Sb$ by using the linearized augmented plane wave method. One of the results of their study is that the band gap is determined by a balance of ionicity and relativistic effects. The covalent bonding in $Li_3Sb$ accounts for the relatively high band gap. Also, $Li_3Sb$ is found to have an indirect gap. The conduction-band minimum is at the edge of the Brillouin zone at *X*. The results for $K_3Sb$ and $Cs_3Sb$ show smaller band gaps due to an increase in ionicity, but $Cs_3Sb$ has a larger band gap than $K_3Sb$ whereas its ionicity is stronger. This countereffect is ascribed to relativistic effects, which are expected to be stronger in the heavier element Cs. The paper included some results on a cubic lattice consisting of $Sb^{3-}$ ions on a positively charged background. The influence of the lattice constant on the band gap is shown clearly. The $Sb^{3-}$ lattice with the $Li_3Sb$ lattice constant has a band gap of the same magnitude as $Li_3Sb$, the $Sb^{3-}$ lattices with the lattice constants of $K_3Sb$ and $Cs_3Sb$ have band-gap values close to zero, which is another indication of the relativistic effects in the compound $Cs_3Sb$. A more recent band-structure calculation[6] on the hexagonal and cubic phases of $K_3Sb$ explained the discrepancy between the band-gap values obtained from optical data and temperature-dependent conductivity measurements.

A good review of photocathode materials has been given by Sommer.[7] The photoemissive properties of alkali antimonides are a consequence of the low work functions of the alkali metals and the related antimonide compounds. The low work functions of these materials make it possible to fabricate even negative electron affinity devices.[8] The escape energy of the electrons from a semiconductor is generally indicated by the electron affinity. Although the electron affinity is the energy gained by adding an electron to the solid, this energy is defined as the energy difference between the bottom of the conduction band and the vacuum level. An electron that absorbs a photon can be excited to the conduction band. Emission of this photoelectron is therefore dependent on the escape barrier between the conduction-band minimum and the vacuum level. For emission of a photoelectron in photoemissive devices, the band gap and the electron affinity are important energy parameters in relation to the red sensitivity and the quantum efficiency of the photon-electron conversion. A negative electron affinity device has the vacuum level in the band gap of the semiconductor; the excitation of a valence-band electron to the conduction band puts this electron in a state with an energy higher than the vacuum level. Upon emission the photoelectron gains kinetic energy when it leaves the solid. It is obvious that this is a good property for a photocathode material. This property has been studied extensively for the alkali antimonides.[9–11]

In general, the alkali antimonides with stoichiometry

 

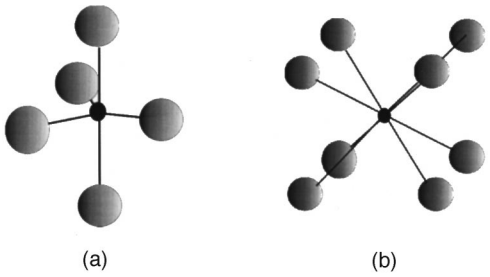


FIG. 1. The coordination of the antimonide atoms in the hexagonal $Na_3Sb$ (a) and cubic $Na_2KSb$ (b) phases. The black spheres represent the Sb atoms and the gray spheres the Na atoms.

$M_3Sb$ (with $M$ an alkali metal atom) appear in two stable phases.[12] The hexagonal phase is most stable for compounds involving alkali metal atoms with relatively small polarizabilities. The cubic phase is favored for compounds involving heavier atoms with a larger polarizability. The crossover occurs at $K_3Sb$ and $Rb_3Sb$. Both compounds are relatively stable in both crystal structures. For $K_3Sb$ the hexagonal phase is slightly more favored and for $Rb_3Sb$ the cubic phase is preferred. $Li_3Sb$ and $Na_3Sb$ are obtained only in the hexagonal phase and $Cs_3Sb$ is cubic. The substitution of one Na atom by K in $Na_3Sb$ to form $Na_2KSb$ leads to a stable cubic phase. It seems likely that the more polarizable K atom stabilizes the cubic structure of this Na-Sb compound.

In this paper, band-structure calculations are presented of the related compounds $Na_2KSb$ and $Na_3Sb$. These calculations are an extension of the work of Wei and Zunger[5] in relation to the application of alkali antimonide compounds in photocathodes. The absence of calculations on the ternary compound $Na_2KSb$ and the influence of the mixing of alkali metals on the band gap and the conduction-band minimum are a gap in the understanding of photoemissive materials applied in photodetetctors.

## II. CRYSTAL STRUCTURES

The coordination of the Sb atoms is very different for the two crystal structures studied. In the hexagonal phase ($Na_3Sb$) the Sb atom is in a trigonal biprismatic coordination with five Na atoms as shown in Fig. 1(a). The fivefold coordination is slightly distorted by the elongation of the bond distances along the $c$ axis. The Na-Sb distances in the Na-Sb plane is 3.09 Å and the Na-Sb distance along the $c$ axis is 3.16 Å. The unit cell dimensions of this structure are $a=5.355$ Å and $c=9.496$ Å, the space group is $P6_3/mmc$ (no. 194), or $D_{6h}^4$ in Schoenflies notation. The Sb atoms occupy the $2c$ Wyckoff position with coordinates $\pm(\frac{1}{3}, \frac{2}{3}, \frac{1}{4})$, the Na atoms in the Na-Sb plane occupy position $2b$ with coordinates $\pm(0, 0, \frac{1}{4})$, and the Na atoms along the $c$ axis occupy position $4f$ with coordinates $\pm(\frac{1}{3}, \frac{2}{3}, u)$; $\pm(\frac{2}{3}, \frac{1}{3}, \frac{1}{2}+u)$ with $u=0.583$.[12,13]

The face-centered cubic phase of $Na_2KSb$ consists of four molecular units per unit cell. Each Sb atom is in an eightfold coordination surrounded by eight Na atoms [see Fig. 1(b)]. The $SbNa_8$ clusters are edge sharing and the K atoms fill the empty holes in the framework. The unit-cell axis of this cubic structure is 7.74 Å. The Na-Sb distance in this structure is 3.35 Å. The space group of this compound is $Fm3m$ (no. 225) or $O_h^4$ in Schoenflies notation. The Sb atoms occupy the Wyckoff position $4a$ with coordinates (0,0,0), the K atoms occupy position $4b$ with coordinates $(\frac{1}{2}, \frac{1}{2}, \frac{1}{2})$, and the Na atoms occupy position $8c$ with coordinates $\pm(\frac{1}{4}, \frac{1}{4}, \frac{1}{4})$.[14,15,16,17]

TABLE I. Input parameters for the calculation of $Na_3Sb$. (ES denotes empty sphere.)

| Atom | Position | Start configuration | Sphere radius (Å) |
|---|---|---|---|
| Na | $2b$ $\pm$(0,0,1/4) | $[Ne]3s^1 3p^0(3d^0)$ | 2.0 |
| Na | $4f$ $\pm$(1/3,2/3,0.583) $\pm$(2/3,1/3.0.083) | $[Ne]3s^1 3p^0(3d^0)$ | 2.0 |
| Sb | $2c$ $\pm$(1/3,2/3,1/4) | $[Kr]5s^2 5p^3 5d^0(4f^0)$ | 1.9 |
| ES | $2a$ (0,0,0); (0,0,1/2) | $1s^0 2p^0(3d^0)$ | 1.0 |

## III. BAND-STRUCTURE CALCULATIONS

The band-structure calculations were done with the localized spherical wave (LSW) method[18] which is adapted from the augmented spherical wave method.[19] Electron exchange and correlation were treated with the local spin-density approximation.[20] Scalar relativistic effects were included.[21] In the LSW program the radial parts of the wave functions are described by a numerical solution of the Schrödinger equation within the spheres and augmented by spherical Hankel functions outside the spheres. On neighboring atom sites the Hankel functions are expanded in series of Bessel functions centered in these neighboring spheres. Around each atom a cluster is formed with wave functions that fall off rapidly with increasing distance from the central atom.

The basis functions of the Na sites were composed of $s$ and $p$ Hankel functions representing the $3s$ and $3p$ valence states. The overlapping wave functions of neighboring atoms were taken into account by $s$, $p$, and $d$ Bessel functions. For the Sb and K atoms $s$, $p$, and $d$ Hankel functions and $s$, $p$, $d$, and $f$ Bessel functions were included in the calculations. Despite the higher packing density of the hexagonal phase an empty sphere had to be included for the calculations on $Na_3Sb$. The input parameters are listed in Table I for $Na_3Sb$ and in Table II for $Na_2KSb$.

## IV. RESULTS

The dispersion of the energy bands in $Na_3Sb$ is shown in Fig. 2. The points in reciprocal space and the first Brillouin zone are drawn in Fig. 3. The most characteristic property in the electronic structure becomes apparent when the dispersive electron states of the conduction-band minimum are compared with the state densities shown in Fig. 4. This band,

TABLE II. Input parameters for the calculation of $Na_2KSb$.

| Atom | Position | Start configuration | Sphere radius (Å) |
|---|---|---|---|
| Na | $8c$ $\pm$(1/4,1/4,1/4) | $[Ne]3s^1 3p^0(3d^0)$ | 1.6 |
| K | $4b$ (1/2,1/2,1/2) | $[Ar]4s^1 4p^0 3d^0(4f^0)$ | 2.0 |
| Sb | $4a$ (0,0,0) | $[Kr]5s^2 5p^3 5d^0(4f^0)$ | 2.4 |

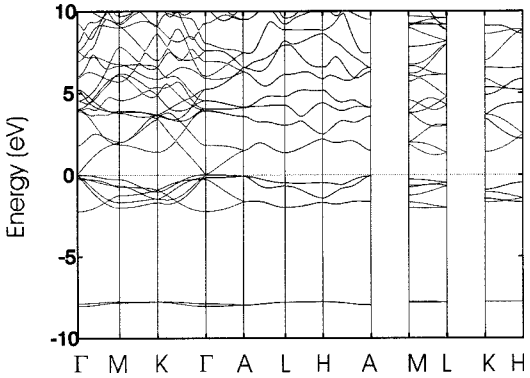


FIG. 2. The dispersion curves for the electronic energy bands in $Na_3Sb$.

consisting of Na $3s$ states, disperses strongly near the center of the Brillouin zone and involves only a small number of electron states. These states are sufficient in number to determine the electrical conductivity properties of this compound. However, the density of these states is far too low to generate any appreciable optical absorption. The very low state density at the bottom of the conduction band has given rise to a discrepancy in the band-gap values found from conductivity and optical absorption measurements. The calculated energy, orbital character, and symmetry of the eigenvectors in the center of the Brillouin zone are listed in Table III.

The bands with the lowest energy are mainly composed of the Sb $5s$ states. The low energy and the small dispersion of these states indicate its localized character and small contribution to the bonding. The valence bands are rather narrow with a width of only 2.5 eV. The lowest bands are nondegenerate at the $\Gamma$ point and have Sb $5p_z$ orbital character. These two bands also show considerable dispersion in the $\Gamma A$ direction, leading to a twofold degeneracy at point $A$ of the first Brillouin zone. The Sb $5p_x$ and $5p_y$ orbitals form bands that are twofold degenerate at $\Gamma$ and are dispersive in the $xy$ plane. The conduction-band minimum is a band from Na $3s$ states which are centered at the $4f$ positions. This highly symmetric band is strongly dispersive in all directions in $k$ space and has its energy minimum just above the valence-band maximum at $\Gamma$. This dispersive behavior is the reason for the very low density of states at the bottom of the conduction band. The second conduction band with energy $+1.85$ eV at $\Gamma$ has its main contribution from the Na $3s$ states located in the hexagonal Na-Sb plane. The Na $3p$ and Sb $5d$ states have higher energies. The photon absorption in the optical region is dominated by the Sb $5p$ to Na $3s$ transitions. Regarding symmetry, the $\Gamma_1^+$ and $\Gamma_4^-$ of the Na $3s$ states in the center of the Brillouin zone, these bands are dipole-allowed final states from the Sb $5p$ valence-band initial states.

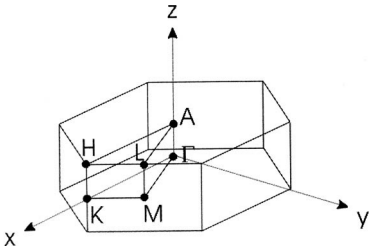


FIG. 3. The first Brillouin zone of $Na_3Sb$ and the high-symmetry points of the irreducible part of this zone.

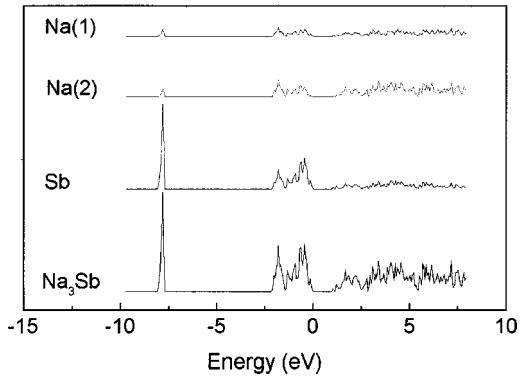


FIG. 4. Densities of states for the constituents in $Na_3Sb$. Na(1) refers to the Na atoms in the hexagonal Na-Sb plane, and Na(2) to the Na atoms that are on the top and bottom of the trigonal bipyramid.

The dispersion of the electron bands of the cubic $Na_2KSb$ structure is shown in Fig. 5, the high-symmetry points in the first Brillouin zone of reciprocal space are drawn in Fig. 6, and the densities of states for the constituents in Fig. 7. The number of bands in the cubic structure is less due to the smaller primitive unit cell with only one $Na_2KSb$ unit. The lowest band is an Sb $5s$ band with an energy of 7.9 eV below the Fermi level at $\Gamma$. The valence bands are mainly Sb $5p$ states and the three Sb $5p$ bands are threefold degenerate in the center of the Brillouin zone where the bands have their highest energy. The conduction band has its minimum also in the center of the Brillouin zone. This band of Na $3s$ and K $4s$ states is a dipole-allowed final state for optical excitations from the valence band. The other conduction bands are the $d$ bands of Sb and K with $t_{2g}$ and $e_g$ symmetry. These bands are accessible from the valence band for dipole transitions in the blue and (ultra)violet region of the optical spectrum.

The calculated energy, orbital character, and symmetry in the center of the Brillouin zone for $Na_2KSb$ are shown in Table IV.

TABLE III. Energy, symmetry (Ref. 22), and main orbital character of the electron bands in the center of the Brillouin zone of $Na_3Sb$ between $-10$ and $+5$ eV binding energy.

| Energy (eV) | Symmetry | Orbital character |
|---|---|---|
| $-8.04$ | $\Gamma_1^+$ | Sb $5s$ |
| $-7.87$ | $\Gamma_4^-$ | Sb $5s$ |
| $-2.24$ | $\Gamma_3^+$ | Sb $5p_z$ |
| $-0.27$ | $\Gamma_2^-$ | Sb $5p_z$ |
| $-0.16$ | $\Gamma_6^+$ | Sb $5p_{xy}$ |
| $-0.02$ | $\Gamma_5^-$ | Sb $5p_{xy}$ |
| $+0.05$ | $\Gamma_1^+$ | Na $3s$ |
| $+1.82$ | $\Gamma_4^-$ | Na $3s$ |
| $+3.92$ | $\Gamma_3^+$ | Na $3p_z$, $3s$ |
| $+3.96$ | $\Gamma_2^-$ | Na $3s$, $3p_z$ |
| $+4.05$ | $\Gamma_5^-$ | Na $3p_{xy}$ |
| $+4.55$ | $\Gamma_6^+$ | Na $3p_{xy}$ |

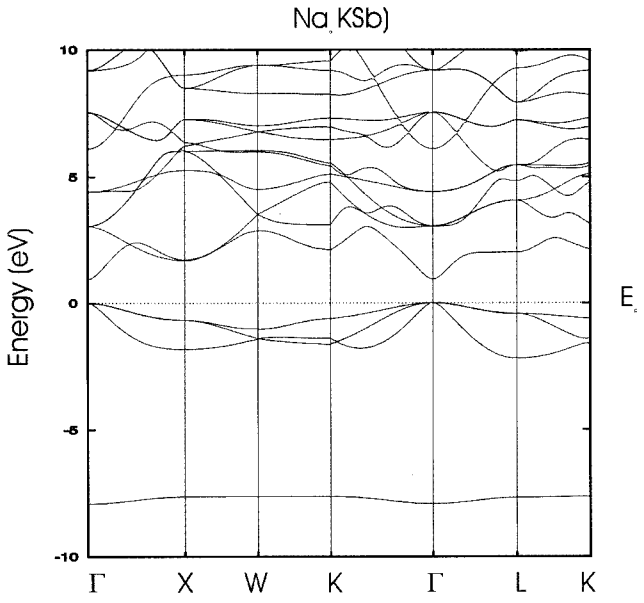


FIG. 5. The dispersion curves for the electronic energy bands in $Na_2KSb$.

## V. DISCUSSION AND CONCLUSION

The low density of states at the bottom of the conduction band in hexagonal $Na_3Sb$ is very similar to that in the hexagonal and cubic phases of $K_3Sb$.[6] The strong dispersion of the lowest conduction band in $Na_3Sb$ and $K_3Sb$ is in good agreement with the LMTO calculations of Tegze and Hafner.[3] This low electron state density led to a discrepancy in band-gap values determined from optical data and temperature-dependent conductivity measurements. Although band-gap values calculated within the local density approximation are often underestimated,[23,24] the band-gap values calculated for $K_3Sb$ are in good agreement with experimental data.[6] From the dispersion curve of the lowest conduction band (Fig. 2) in $Na_3Sb$ and the density of states (Fig. 4) it becomes clear that $Na_3Sb$ also has a delayed optical absorption onset. Although conductivity data are not available for $Na_3Sb$ the optical absorption data show an absorption onset at a photon energy of about 0.7 eV.[1] This is in fair agreement with the value of 0.9 eV derived from Fig. 4. The band gap determined from the energies of the eigenvectors at $\Gamma$ is 0.07 eV, which is an order of magnitude less.

In contrast to the monoalkali antimonides, the bialkali antimonide $Na_2KSb$ does show a much smaller discrepancy between the absorption onset and the band-gap value. The energy gap determined from the eigenvectors is 0.9 eV and it is 1.4 eV from the density of states. Unfortunately, temperature-dependent conductivity data are not available for this compound, but experimental photon absorption data indicate a band gap of 1.0 eV.[1]

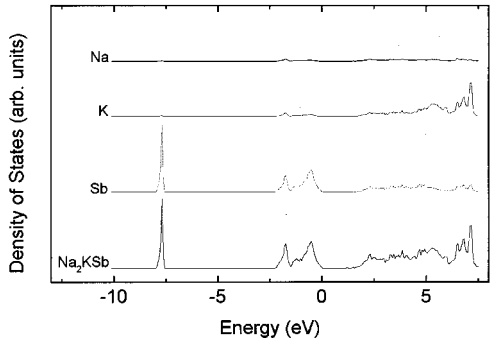


FIG. 7. Densities of states for the constituents in $Na_2KSb$.

The smaller discrepancy in the band-gap values for the bialkali antimonide $Na_2KSb$ is likely the reason for its better performance with respect to the monoalkali antimonides as a photocathode in photoemissive devices. The conduction-band electrons generated by optical transitions in the monoalkali antimonides can lose much energy by phonon emission. The potential barrier for the photoelectrons to escape from the bottom of the conduction band in the solid into the vacuum therefore becomes larger. The bialkali antimonide $Na_2KSb$ has a conduction-band minimum with a higher energy. Electrons excited to this conduction band face a lower escape barrier and are more easily emitted from the solid. This results in a much higher photoemission current for a similar irradiation.

Moreover, the K and Sb $d$ bands with $t_{2g}$ and $e_g$ symmetry are within the range of optical transitions in the blue and (ultra)violet part of the spectrum. Valence-band electrons excited to these final states can easily be emitted because the final-state energy is higher than the escape barrier (work function) of the material. These bands are therefore very important in the photoemission process of photocathodes.

In conclusion, we have calculated the electronic band structures of $Na_3Sb$ and $Na_2KSb$. The strong dispersive band above the Fermi level causes a discrepancy in the experimental band-gap values. In the bialkali antimonide $Na_2KSb$ this

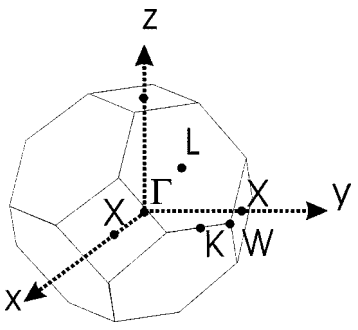


FIG. 6. The first Brillouin zone of $Na_2KSb$ and the high-symmetry points of the irreducible part of this zone.

TABLE IV. Energy, symmetry (Ref. 22), and main orbital character of the electron bands in the center of the Brillouin zone of $Na_2KSb$ between $-10$ and $+10$ eV binding energy.

| Energy (eV) | Symmetry | Orbital character |
|---|---|---|
| −7.92 | $\Gamma_1^+$ | Sb 5$s$ |
| 0.00 | $\Gamma_4^-$ | Sb 5$p$ |
| +0.93 | $\Gamma_1^+$ | Na 3$s$, K 4$s$ |
| +3.04 | $\Gamma_5^+$ | Sb 5$d$, K 3$d$ ($t_{2g}$) |
| +4.40 | $\Gamma_3^+$ | Sb 5$d$, K 3$d$ ($e_g$) |
| +6.09 | $\Gamma_2^-$ | Na 3$s$ |
| +7.52 | $\Gamma_4^-$ | K 4$p$ |
| +9.17 | $\Gamma_5^+$ | Sb 5$d$, K 3$d$ ($t_{2g}$) |

band is less dispersive and the conduction-band minimum is at a higher energy. Electrons excited to the conduction bands in $Na_2KSb$ experience a much smaller barrier to overcome the vacuum level than do electrons that can relax by phonon emission to energies just above the valence band (as is the case in the monoalkali antimonides). This is a likely reason why the bialkali antimonide $Na_2KSb$ is applied so successfully in photoemissive devices.

**ACKNOWLEDGMENTS**

This work was supported by the Stichting voor Fundamenteel Onderzoek der Materie (FOM) with financial support from the Nederlandse Organisatie voor Wetenschappelijk Onderzoek (NWO) and by the Technology Foundation STW, Applied Science division of NWO, and the technology program of the Ministry of Economic Affairs.

*Electronic address: ettema@tn.tudelft.nl

[1] W. E. Spicer, Phys. Rev. **112**, 114 (1958).
[2] A. H. Sommer, Rev. Sci. Instrum. **26**, 725 (1955).
[3] M. Tegze and J. Hafner, J. Phys.: Condens. Matter **4**, 2449 (1992).
[4] E. V. Chulkov, O. S. Koroleva, and V. M. Silkin, in *Proceedings of the 20th International Conference on the Physics of Semiconductors*, edited by E. M. Anastassakis and J. D. Joannopoulos (World Scientific, Singapore, 1990), Vol. 3, p. 1743.
[5] S. H. Wei and A. Zunger, Phys. Rev. B **35**, 3952 (1987).
[6] A. R. H. F. Ettema and R. A. de Groot, J. Phys.: Condens. Matter **11**, 759 (1999).
[7] A. H. Sommer, *Photoemissive Materials*, reprinted ed. (Krieger, New York, 1980).
[8] R. L. Bell, *Negative Electron Affinity Devices* (Clarendon, Oxford, 1973).
[9] B. Erjavec, Appl. Surf. Sci. **103**, 343 (1996).
[10] T. Guo and H. Gao, Appl. Phys. Lett. **58**, 1757 (1991).
[11] T. Guo and H. Gao, Appl. Surf. Sci. **70/71**, 355 (1993).
[12] R. W. G. Wyckoff, *Crystal Structures* (Wiley, New York, 1960), Vol. 2.
[13] G. Brauer and E. Zintl, Z. Phys. Chem. Abt. B **37**, 323 (1937).
[14] J. Chikawa, S. Imamura, K. Tanaka, and M. Shiojiri, J. Phys. Soc. Jpn. **16**, 1175 (1961).
[15] J. J. Scheer and P. Zalm, Philips Res. Rep. **14**, 143 (1959).
[16] W. H. McCarroll, J. Phys. Chem. Solids **16**, 30 (1960).
[17] W. H. McCarroll and R. E. Simon, Rev. Sci. Instrum. **35**, 508 (1964).
[18] H. van Leuken, A. Lodder, M. T. Czyzyk, F. Springelkamp, and R. A. de Groot, Phys. Rev. B **41**, 5613 (1990).
[19] A. R. Williams, J. Kübler, and C. D. Gelatt, Phys. Rev. B **19**, 6094 (1979).
[20] L. Hedin and B. Lundqvist, J. Phys. C **4**, 2064 (1971).
[21] M. Methfessel and J. Kübler, J. Phys. F: Met. Phys. **12**, 141 (1982).
[22] We use the symmetry notation of G. F. Koster, J. O. Dimmock, R. G. Wheeler, and H. Statz, *Properties of the Thirty-Two Point Groups* (MIT Press, Cambridge, MA, 1963).
[23] A. Zunger and M. L. Cohen, Phys. Rev. B **18**, 5449 (1978).
[24] J. P. Perdew and Z. Zunger, Phys. Rev. B **23**, 5048 (1981).